ACS OMEGA

http://pubs.acs.org/journal/acsodf
Article

Synergistic Effect of Styrene and Carbon Black on the Fatigue Properties of Styrene−Butadiene Rubber Composites

Li'e Wang, Zhu Luo,* Le Yang, Jincheng Zhong, and Yinhan Xu

Cite This: *ACS Omega* 2024, 9, 2000−2011
Read Online

ACCESS | Metrics & More | Article Recommendations

ABSTRACT: The increase in the styrene content in styrene−butadiene rubber (SBR) can improve the abrasion performance and cutting resistance of rubber, which has received attention in the tire industry. The fatigue performance is the main evaluation index of rubber materials applied to tires. In this study, the effect of the styrene content and its interaction with carbon black (CB) on the dynamic fatigue performance and mechanism of SBR were investigated. The results indicated that the dynamic fatigue life of the rubber composite materials was prolonged with increasing styrene content; furthermore, it showed a trend of increasing and then decreasing with increasing CB content. At a certain CB content, styrene and CB displayed a synergistic effect on improving the dynamic fatigue life of the composite materials. The dynamic fatigue performance of SBR_{40}/CB_{20} was the best. The expansion of the fatigue cracks followed the secondary cracking mechanism, which consumed a large amount of strain energy and slowed the development of the main crack. However, when the CB content exceeded 40 phr, the mechanism transformed to main crack self-propagation and the fatigue life decreased.

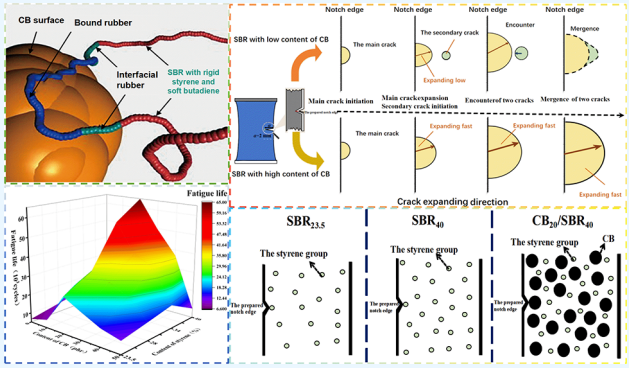

1. INTRODUCTION

Styrene−butadiene rubber (SBR) is a random copolymer of butadiene and styrene and has become one of the most widely used synthetic rubbers because of its excellent processability, wear resistance, and aging resistance. Especially in the field of construction machinery and underground mining, due to the rigidity of the styrene group and its low hysteresis to give SBR good puncture and cut resistance, SBR has become the mainstream engineering tire tread rubber. The study of styrene groups on the rheological behavior and antifatigue properties of SBR is important to improve the performance of engineering tires further. It has been reported that the cutting resistance and puncture resistance of SBR can be improved by increasing its styrene content,[1−4] but the influence of styrene content on the fatigue performance has not been reported.

The fatigue performance of rubber materials generally refers to the process in which the material is subjected to alternating stress (strain), and microscopic damage occurs on the surface or inside the material under a certain cyclic loading; thus, the material properties are gradually weakened in the application process due to the continuous development of fatigue damage. This process causes permanent structural damage and causes the product to fail. The fatigue resistance of rubber materials applied to tires has a significant effect on their safety and reliability; therefore, it is of great significance to study the fatigue performance of SBR and develop novel types of SBR materials with excellent fatigue resistance. Researchers have focused on the fatigue behavior of rubber materials, primarily focusing on the initiation, development, and termination of fatigue cracks;[5−9] fatigue damage evolution and fatigue crack growth;[10−13] the relationship between fatigue life and tearing energy or strain energy density;[14−16] and improving the fatigue resistance of rubber.[17−19] Dong et al.[20−22] investigated the effects of carbon black (CB) and nano-CB on the fatigue properties of rubber materials. Weng et al.[23−25] studied the fatigue behavior of CB-filled or silica-filled rubber and discussed the relationship between tear energy and fatigue properties of rubber. Yin et al.[26] studied the effect of silica modified by different methods on the fatigue behavior of dissolved polystyrene butadiene rubber. Fu et al.[27] explored the effect of silica particle size and functional groups on fatigue crack development in natural rubber. Luo and co-workers[28−31] studied fatigue crack growth in aramid fiber-reinforced SBR composites. Adding CB is a common method to improve the

Received: December 10, 2023
Revised: December 18, 2023
Accepted: December 25, 2023
Published: December 29, 2023

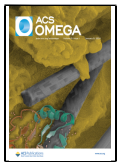

https://doi.org/10.1021/acsomega.3c09872
ACS Omega 2024, 9, 2000−2011

strength of the SBR in the rubber industry. To improve its fatigue properties, rubber enterprises have developed many varieties of SBR. As one of the components of SBR macromolecules, the content of styrene, especially its interaction with CB, may have a significant impact on fatigue performance, but as far as we know, there is no research report at present.

Many researchers are focusing on compounding CB with other reinforcement systems to further improve the performance of the SBR tires. Kaynak[32] partially replaced CB with feldspar to reinforce SBR and found that the incorporation of treated feldspar resulted in the formation of a smaller filler network enhancing the filler−polymer interaction, with better rolling resistance and winter traction performance of the tires. Li[33] introduced crystalline trans-1,4-poly(butadiene-*co*-isoprene) into the tread rubber system of off-road tires and found that the aggregation structure of the CB-filled tread rubber alone was improved, which led to the improvement of the new system's tread rubber in terms of heat accumulation, rolling resistance, abrasion resistance, and fatigue resistance. In terms of tire life, the development of fatigue cracks leads to tire failure and is one of the causes of tire blowouts. SBR is a low-strength synthetic rubber and is the main rubber of engineering tire treads. CB is the most common rubber filler, especially for SBR. Engineering tires are often punctured by sharp stones, which introduce cracks on their surfaces, and the continuous development of cracks causes the tire to fail eventually. In this work, the dynamic fatigue behavior and mechanism of the notched SBR/CB samples with different contents of styrene and CB are studied. The influences of the contents of styrene in the SBR matrix and CB filler as well as their synergistic interaction on the rheological behaviors are explored, and the crack extension behavior in strain-controlled fatigue is also investigated. These research results can guide the tread formulation design of engineering tires and are of great significance to study the fatigue properties of rubber composite materials.

2. EXPERIMENTAL SECTION

2.1. Materials. SBR 1500E (styrene of 23.5%) and SBR 1586 (styrene of 40.0%) were obtained from PetroChina Lanzhou Petrochemical Company. CB (N330) was provided by Jiangxi Heimao Industry Co. Ltd. Zinc oxide (ZnO) was acquired from Jiangsu Tianli Zinc Industry Co. Ltd., China. Stearic acid (SA) was purchased from Nantong Kaita Chemical Co. Ltd., China. Sulfur (S8) was provided by Guiyang Hangyi Rubber and Plastic Accessories Co. Ltd., China. The accelerant, N-*tert*-butyl-2-benzothiazole sulfenamide (TBBS), was purchased from Shandong Shangshun Chemical Co. Ltd., China.

2.2. Preparation of Composites. An open mixer (XSS-300, Shanghai Kechuang Rubber & Plastic Machinery Equipment Co. Ltd., China) was used to mix SBR1586 and SBR1500E in different ratios, and then four kinds of rubber with styrene contents of 23.5, 28, 34, and 40% were obtained. The detailed formulations are listed in Table 1. Second, rubber composites were obtained by mixing SBR_{xx}, CB_n, and other rubber auxiliaries, where the subscripts "*xx*" and "*n*" represented the percentage of styrene in the mixed rubber and the percentage of CB in the composites, respectively. The composite formulations are given in Table 2. The compound rubber was placed for 24 h to relieve stress and then cured at 151 °C for 40 min on a vulcanizing press.

Table 1. Sample Formulation

sample	$SBR_{23.5}$	SBR_{28}	SBR_{34}	SBR_{40}
SBR1500E (g)	800	582	291	0
SBR1586 (g)	0	218	509	800

Table 2. Formulation of the Composites

sample	SBR_{xx}	N330	ZnO(g)	SA(g)	S(g)	TBBS(g)
SBR_{xx}	800	0	24	8	14	8
SBR_{xx}/CB_{10}	800	80	24	8	14	8
SBR_{xx}/CB_{20}	800	160	24	8	14	8
SBR_{xx}/CB_{30}	800	240	24	8	14	8
SBR_{xx}/CB_{40}	800	320	24	8	14	8
SBR_{xx} /CB_{50}	800	400	24	8	14	8

2.3. Characterization. *2.3.1. Testing of Strain Scanning.* The storage modulus (G') of the compound rubber as a function of strain was tested by a rubber processing analyzer (RPA2000, ALPHA, USA). The specimen shape had a diameter of 4.5 cm and a thickness of 2 mm. The test conditions are as follows: the temperature was 100 °C, the frequency was 1 rad/s, and the strain range was 0.01−100%.

2.3.2. Testing of Frequency Scanning. The loss factor (tan δ) of the compound rubber as a function of frequency was tested by a rubber processing analyzer (RPA2000, ALPHA, USA). The specimen shape had a diameter of 4.5 cm and a thickness of 2 mm. The test conditions are as follows: the temperature was 100 °C, the strain was 20%, and the frequency was 1−15 Hz.

2.3.3. Dynamic Mechanical Analysis. A dynamic mechanical analyzer (Q800, TA Instruments, USA) was applied to obtain the glass-transition temperature (GTT) of the rubber sample. The frequency and amplitude were set at 1.0 Hz and 20 μm, respectively. The temperature sweep range was from −70 to +70 °C, with a heating rate of 3 °C·min^{-1}.

2.3.4. Dynamic Fatigue Test. A single-edge notched fatigue specimen of the vulcanized SBR is shown in Figure 1.

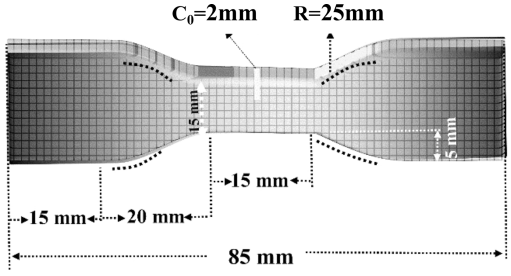

Figure 1. Notched fatigue specimen diagram.

The specimens were made into 2 mm precuts at the center of one edge by a new razor blade, thus producing single-edge notched test pieces. The tensile fatigue cycle test was conducted on a dynamic fatigue machine (DF-8000-5, High Iron Detection Instruments, Dongguan Co. Ltd, Guangdong, China). The test conditions are as follows: In strain control mode and sinusoidal loading, the specimen was prestretched for 5 mm, the cyclic displacement was ±5 mm, the elongation was 67%, and the frequency was 5 Hz. The tensile fatigue crack length was observed by a magnifying glass (PEAK1983-15 X,

https://doi.org/10.1021/acsomega.3c09872
ACS Omega 2024, 9, 2000−2011

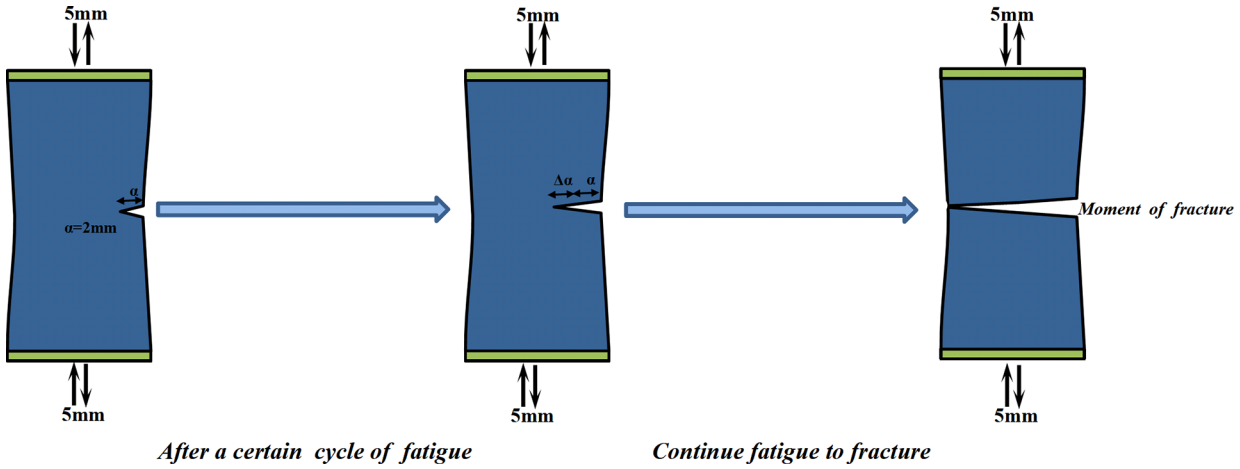

Figure 2. Schematic for crack growth of SBR during the dynamic fatigue process.

PEAK, Japan) every 2500 fatigue cycles. More than five fatigue crack length tests were performed on each set of specimens, and only three sets with stable data were selected for analysis.

2.3.5. Determination of Dynamic Fatigue Fracture Morphology. Scanning electron microscopy (SEM, JSM-7500F, JEOL, Japan) was used to measure the fracture morphology of the fatigue specimens. The working voltage was 10 kV. Before observation, the specimens were pasted onto conductive tape and treated with gold spraying.

2.3.6. Determination of Dynamic Fatigue Crack Tip Morphology. Fatigue specimen: The vulcanized SBR_{40}/CB_{20} and SBR_{40}/CB_{50} were cut into the shape shown in Figure 1 for fatigue testing. The fatigue number was 10,000 or 2500 times, and the specimen was broken along the prefabrication incision after being immersed in liquid nitrogen for 4 h. The morphology of the dynamic fatigue crack tip of the fatigue specimen was observed by SEM.

2.3.7. Tearing Energy and Crack Growth Rate. Rivlin and Thomas[34] proposed that the crack growth rate is related to the tearing energy and independent of the specimen geometry, indicating that the critical tearing energy can be considered an internal property of the rubber material. The tear energy (T) of a single-incision tensile specimen is described as

$$T = 2KUc_0K = \pi/\sqrt{\lambda}$$

where K is a geometrical parameter; λ is the elongation ratio, $\lambda = 1 + \varepsilon$, where ε is the tensile strain; U is the strain energy density, which is the integral area of the tensile stress−strain curve after the Mullins effect is removed; and c_0 is the crack length.

In the dynamic fatigue process, because the tearing energy changes continuously with the change in crack length, the concept of average tear energy is introduced (Figure 2). The average tear energy (T_{av}) for different cycle times is calculated by the following equation:

$$T_{av} = \frac{T_1 + T_2 + \cdots + T_n}{n}$$

where T_1, T_2,..., T_n are the tested tearing energies for every 2500 fatigue cycles.

Grosch[35] found that there was a power exponential relationship between the fatigue crack growth rate and tearing energy when strain was loaded onto a rubber tire reinforced with CB, that is

$$d\alpha/dN = BT^{\beta}$$

where B and β are two parameters related to the materials and fatigue test conditions.

3. RESULTS AND DISCUSSIONS

3.1. Dynamic Thermo-Mechanical Properties. Although the polarity of styrene is very small, its large volume and steric resistance make the butadiene chain segment hard to move, which can be reflected by the temperature corresponding to the tan δ peak, namely, GTT. As shown in Figure 3, the

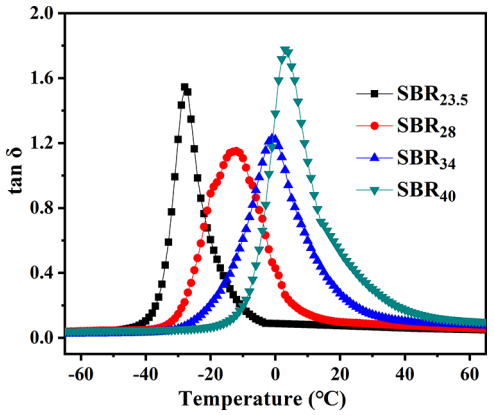

Figure 3. Dynamic mechanical analysis curve of SBR with different styrene content.

internal rotation steric resistance of the molecular chain increases with the increase of styrene content, so that a rise in GTT can be observed. Furthermore, there is only one tan δ peak for each of the four different SBR samples despite the incremental styrene content. The transition peak of styrene copolymer is not found at about 50 °C, further indicating that the four kinds of SBR samples was all styrene and butadiene random copolymers without obvious phase separation structure.

CB is an important reinforcing agent for SBR. As shown in Figure 4, the concentration is diluted, and the force of rubber macromolecules as well as the GTT of SBR/CB composites is reduced with the increase of CB content. In addition, the internal friction among rubber macromolecules and the CB fillers increases owing to the increasing CB, which leads to a

https://doi.org/10.1021/acsomega.3c09872
ACS Omega 2024, 9, 2000−2011

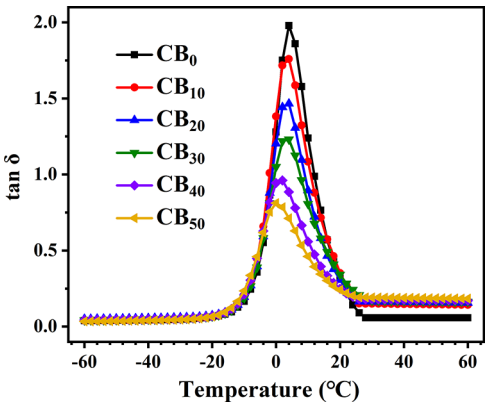

Figure 4. Dynamic mechanical analysis curve of SBR_{40}/CB with different CB content.

rise in the viscosity modulus of SBR/CB composites and an increase in the tan δ value of the composites.

3.2. Viscoelastic Characteristics. The Payne effect is related to the network formed by the filler−filler and filler−rubber interactions. As shown in Figure 5, all of the SBRs with CB_0, CB_{10}, and CB_{20} show a long plateau area for the storage modulus (G') in the smaller strain region. Subsequently, as the strain (γ) increases, the G' value begins to decrease at the critical strain (γ_c). Starting from 40 phr of CB, even at a low strain, G' decreases with increasing strain. It is noteworthy that the decreasing trend increases with increasing CB content and is relatively greater for composites with a high styrene content. The SBR/CB compounds exhibit a significant Payne effect, which becomes increasingly obvious with increasing CB content. The Payne effect also shows an increasing phenomenon with increasing styrene content.[36]

In unfilled rubber, the rubber molecular chains do not untangle at low strain and G' remains constant. When the strain exceeds γ_c, the sliding and untangling of the rubber molecular chains gradually become the dominant factor, with a decline in the G' value. In the small strain area, with increasing CB content, the G' plateau becomes increasingly shorter and the initial G' value of the composites increases. Furthermore, the G' of the composites with high styrene content is higher than that of the composites with low styrene content; this indicates that when the CB content exceeds 30 phr, the interaction between CB and the rubber matrix exhibits defects, and damage to the filler network can occur at a small strain, resulting in a decrease in G'. With increasing CB content, the damage to the filler network also increases correspondingly and the decrease in G' is more obvious. The critical strain of the Payne effect of high styrene content composites decreases as the CB content increases. The G' value of the composites with a high styrene content decreases more significantly, and the Payne effect is more obvious. The weaker the interaction between fillers and rubber, the more obvious the effect is, indicating that with the increase in styrene, the interaction between CB and styrene components is weakened and the reinforced network structure is more sensitive to strain.

Figure 6 shows the relationship plots of tan δ varying with frequency. It can be found that the tan δ value of SBR decreases with the increase of styrene in the whole sweep frequency. On the other hand, the tan δ values of SBR/CB composites increase as the CB content increases, with the effect in the high styrene content sample being more obvious. Because there are more rigid side styrene groups in SBR with

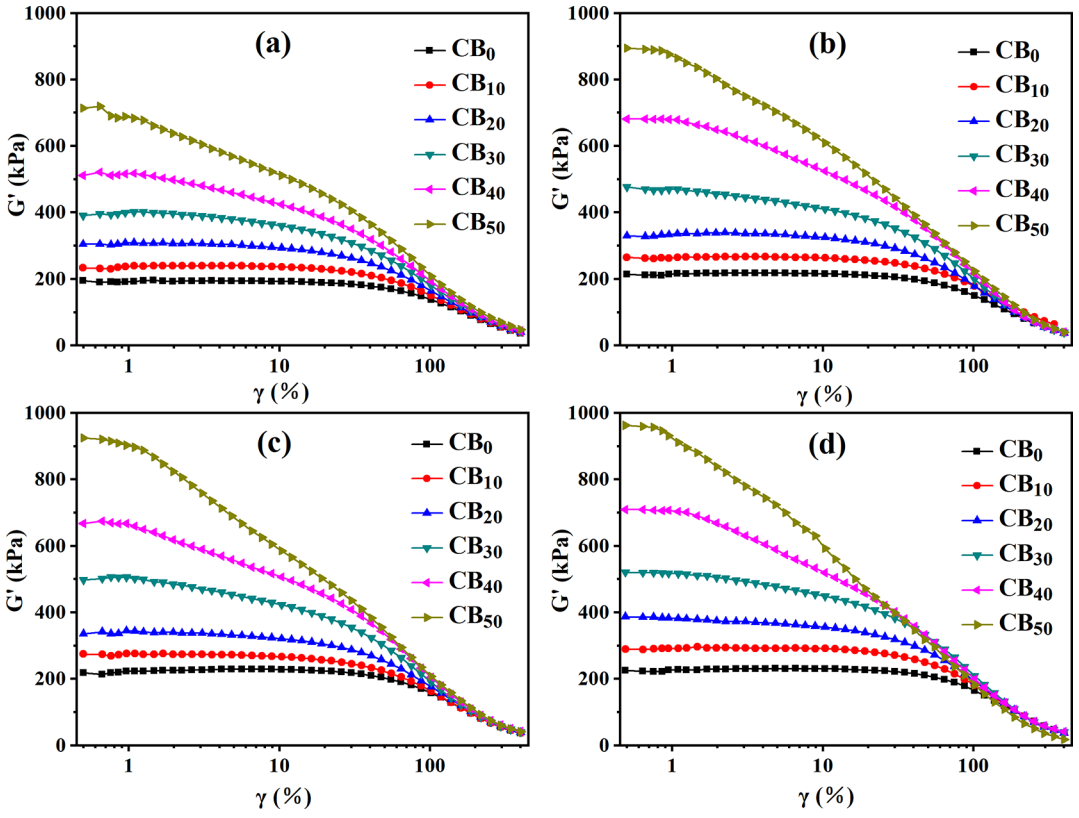

Figure 5. Storage modulus (G') vs strain (γ) plots of different samples. (a) $SBR_{23.5}/CB_n$, (b) SBR_{28}/CB_n, (c) SBR_{34}/CB_n, and (d) SBR_{40}/CB_n.

https://doi.org/10.1021/acsomega.3c09872
ACS Omega 2024, 9, 2000−2011

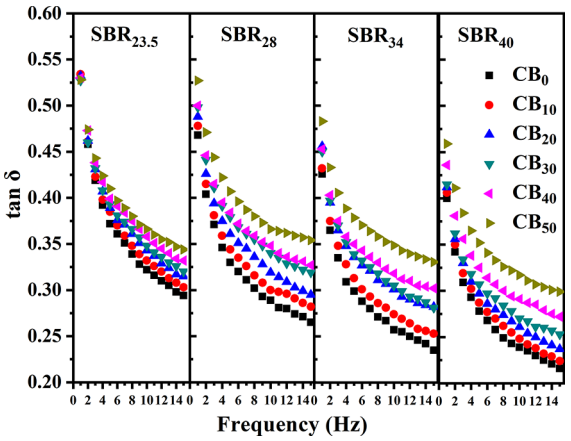

Figure 6. Loss factor (tan δ) vs frequency plots of different samples.

high styrene content, the molecular chains cannot change conformation in time under the action of external forces, resulting in a larger relative energy storage modulus and lower tan δ value. CB and rubber molecules can form CB-rubber gel, which limits the movement of SBR macromolecules, thus the internal friction, loss modulus, and tan δ value are increased. SBR/CB composites with high styrene content have more rigid elements. Under the same macroscopic deformation, the deformation of butadiene flexible elements increases, as a result, more obviously increasing loss modulus and the corresponding tan δ value can be observed.

3.3. Dynamic Fatigue Behaviors of SBR/CB Composites. *3.3.1. Dynamic Fatigue Crack Length of SBR/CB Composites with Different Styrene Contents.* As shown in Figures 7 and 8, the dynamic fatigue crack length of SBR/CB composites increases exponentially with the number of fatigue cycles. For the same CB content, the fatigue life of the

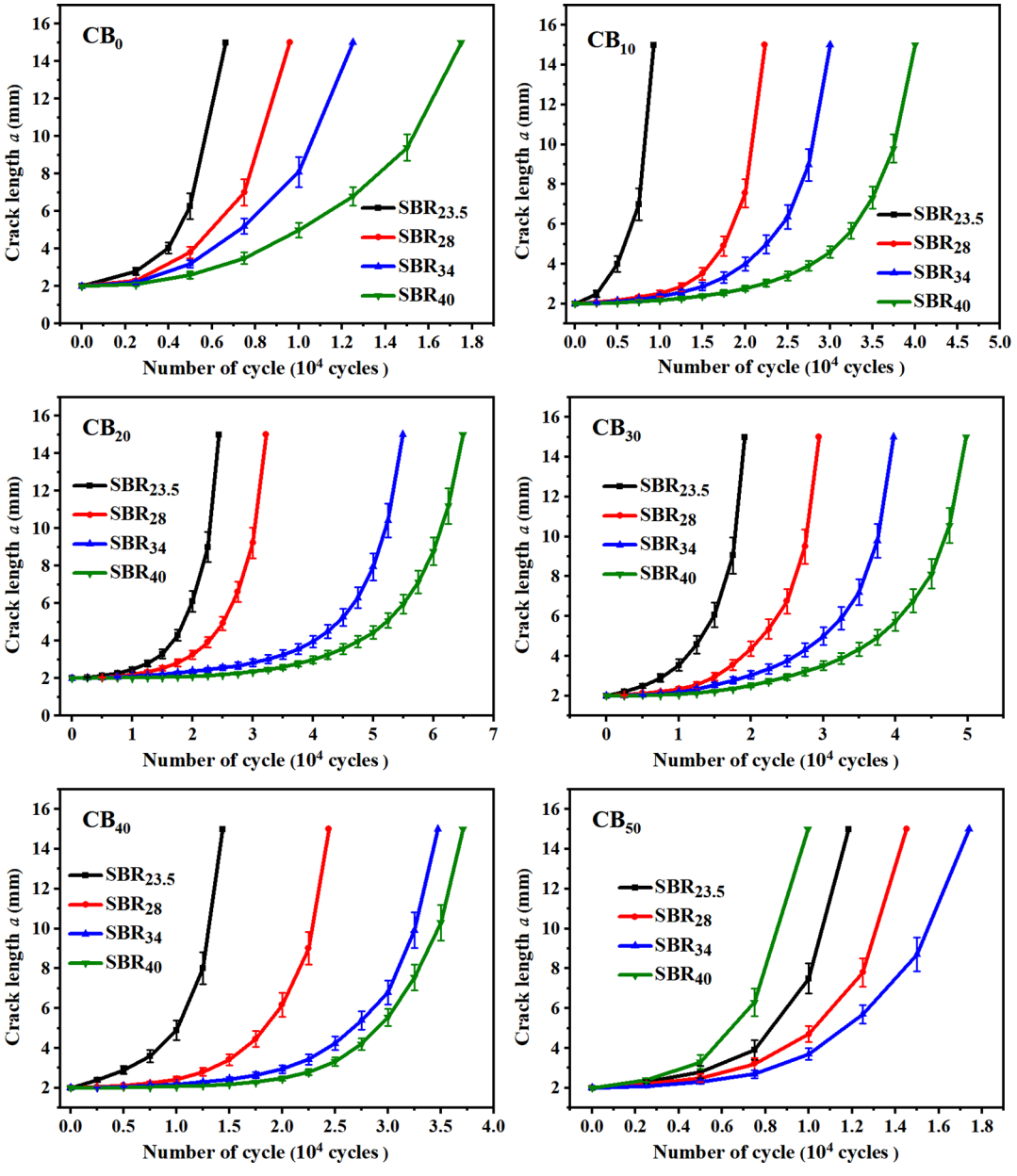

Figure 7. Dynamic fatigue crack length (α) of SBR/CB vs fatigue cycle with different styrene contents.

https://doi.org/10.1021/acsomega.3c09872
ACS Omega 2024, 9, 2000−2011

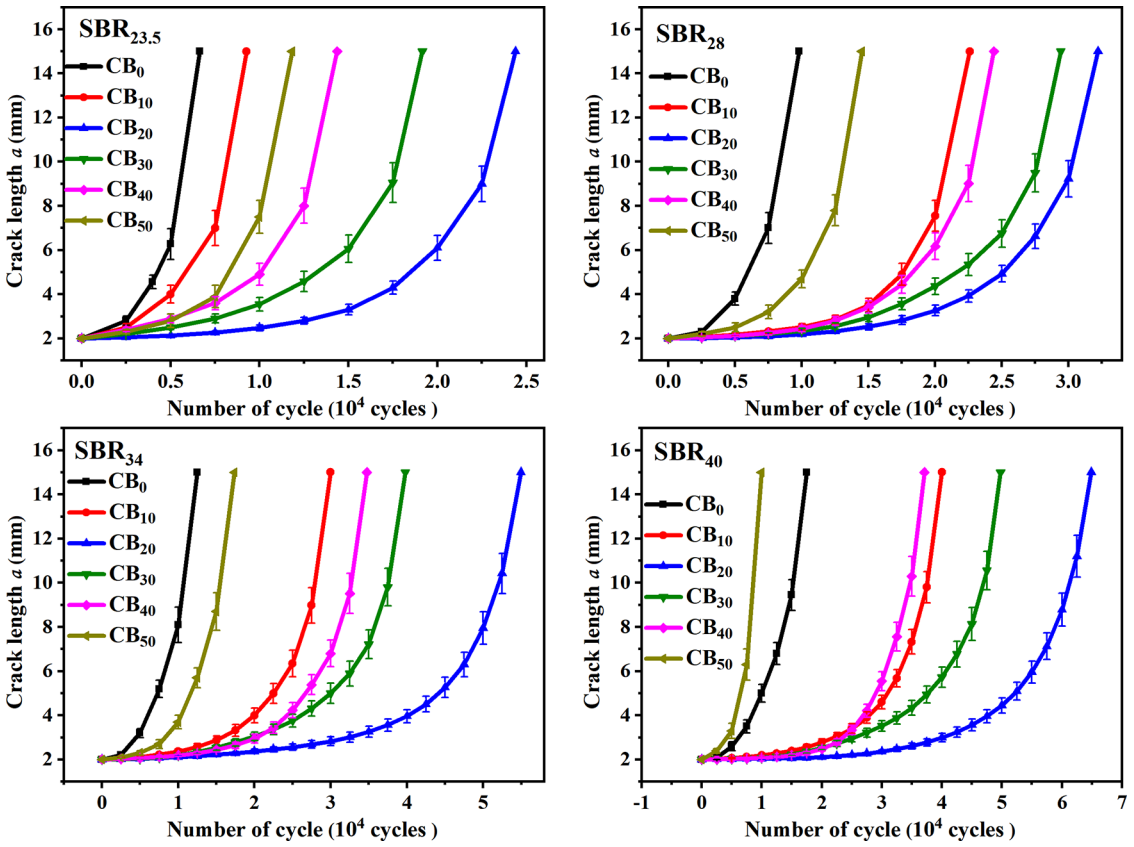

Figure 8. Dynamic fatigue crack length (α) of SBR/CB vs fatigue cycle with different CB contents.

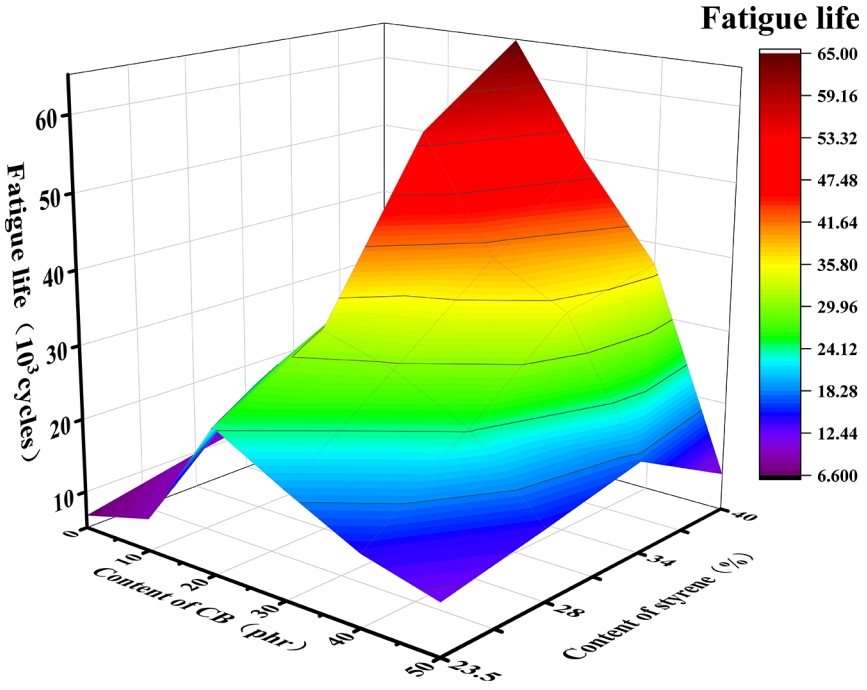

Figure 9. Fatigue life (10^3 cycles) of SBR/CB.

composites increases gradually with increasing styrene content in SBR. In addition, as shown in Figure 8, when the styrene content remains the same, the fatigue life of the rubber composites increases first and then decreases with increasing CB content, and the dynamic fatigue life of SBR/CB_{20} composites is the longest, indicating that CB has a significant influence on the fatigue life. With a further increase in CB content, the slow development stage of cracks is shortened, and the slow development stage disappears when the CB content is 50 phr. This shows that the continuous increase in CB leads to an increase in the number of agglomeration defects, which can accelerate the development of cracks.

https://doi.org/10.1021/acsomega.3c09872
ACS Omega 2024, 9, 2000−2011

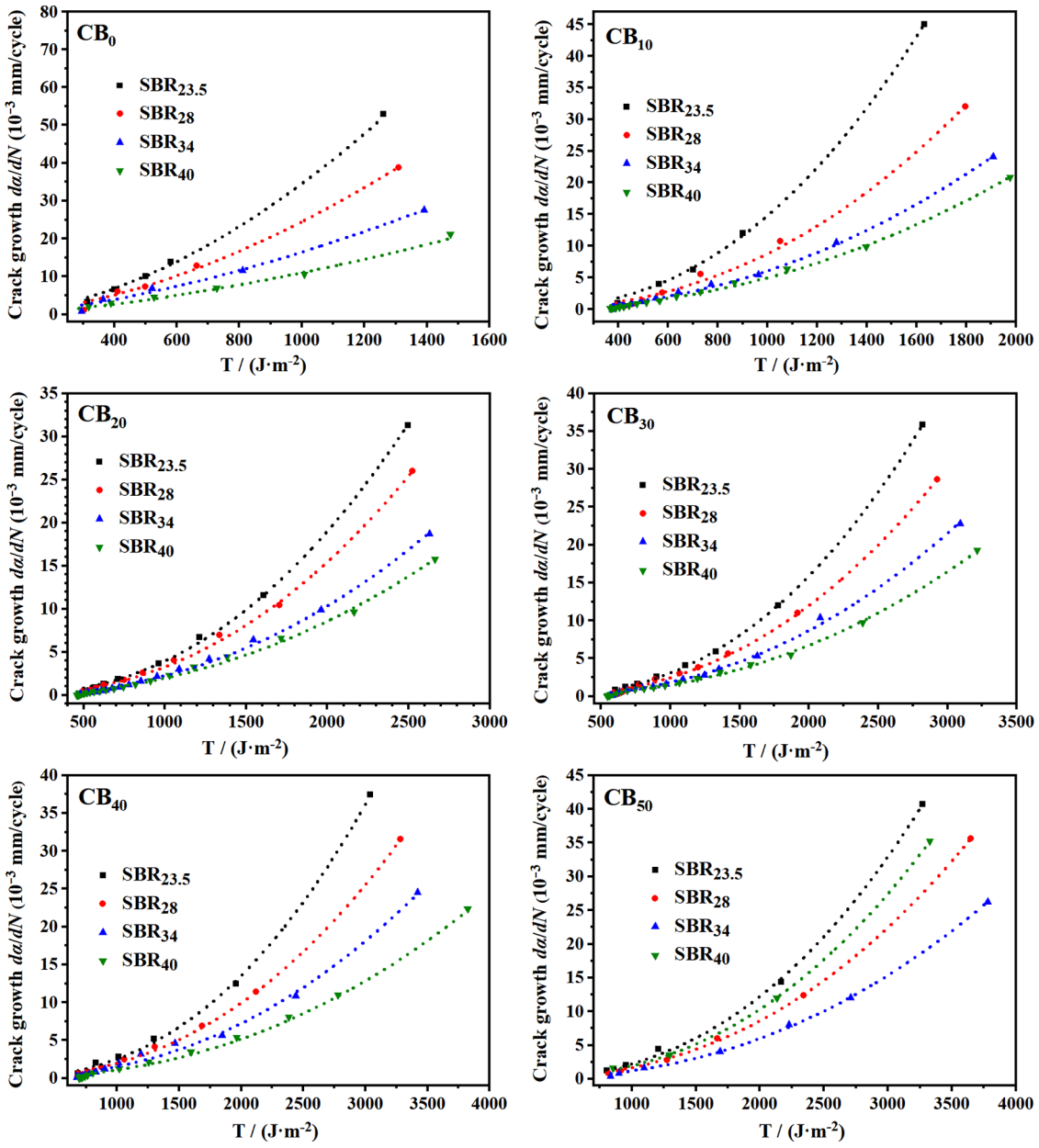

Figure 10. Fitting curve for the dynamic fatigue crack growth rate (dα/dN) vs tearing energy (T) of SBR/CB with different styrene contents.

As shown in Figure 9, compared to $SBR_{23.5}$, the fatigue lives of SBR_{40}, $SBR_{23.5}/CB_{20}$, and SBR_{40}/CB_{20} increase by 200, 264, and 868%, respectively. The synergistic effect of styrene and CB greatly improves the dynamic fatigue properties of the SBR/CB composites.

3.3.2. Relationship between the Dynamic Fatigue Crack Growth Rate and Tearing Energy of SBR/CB Composites with Different Styrene Contents. Figure 10 shows the dynamic fatigue crack growth rate dα/dN as a function of tearing energy T of SBR/CB composites with different styrene contents at 0, 10, 20, 30, 40, and 50 phr CB contents. It can be seen that notched specimens cannot prevent crack propagation when the tearing energy reaches a certain value, the fatigue crack growth rate increases with increasing tearing energy and dα/dN displays a power function relation to T, but the crack growth rate at the same tear energy obviously decreases with an increase in styrene content.

As shown in Figure 11, with increasing CB content, the initial tearing energy of crack growth increases, the slow crack development stage is first extended and then shortened, and the slow crack development stage is the longest at 20 phr of CB. These results show that the addition of CB can significantly increase the strength of the matrix.

It can be observed from Figure 11 that the plots of SBR/CB samples display a power function relationship, which can be expressed by

$$d\alpha/dN = bT^c$$

The b velocity has a great impact on the slow increase in the crack growth rate in the platform region at the initial fatigue stage, where c is the power of the power function, determining the dependence of dα/dN on the tear energy. As shown in Table 3, CB_0 possesses the highest b value of 10^{-4}, which is much higher than that of the other groups. Therefore, the slow crack development phase of CB_0 is too short for it to be

https://doi.org/10.1021/acsomega.3c09872
ACS Omega 2024, 9, 2000−2011

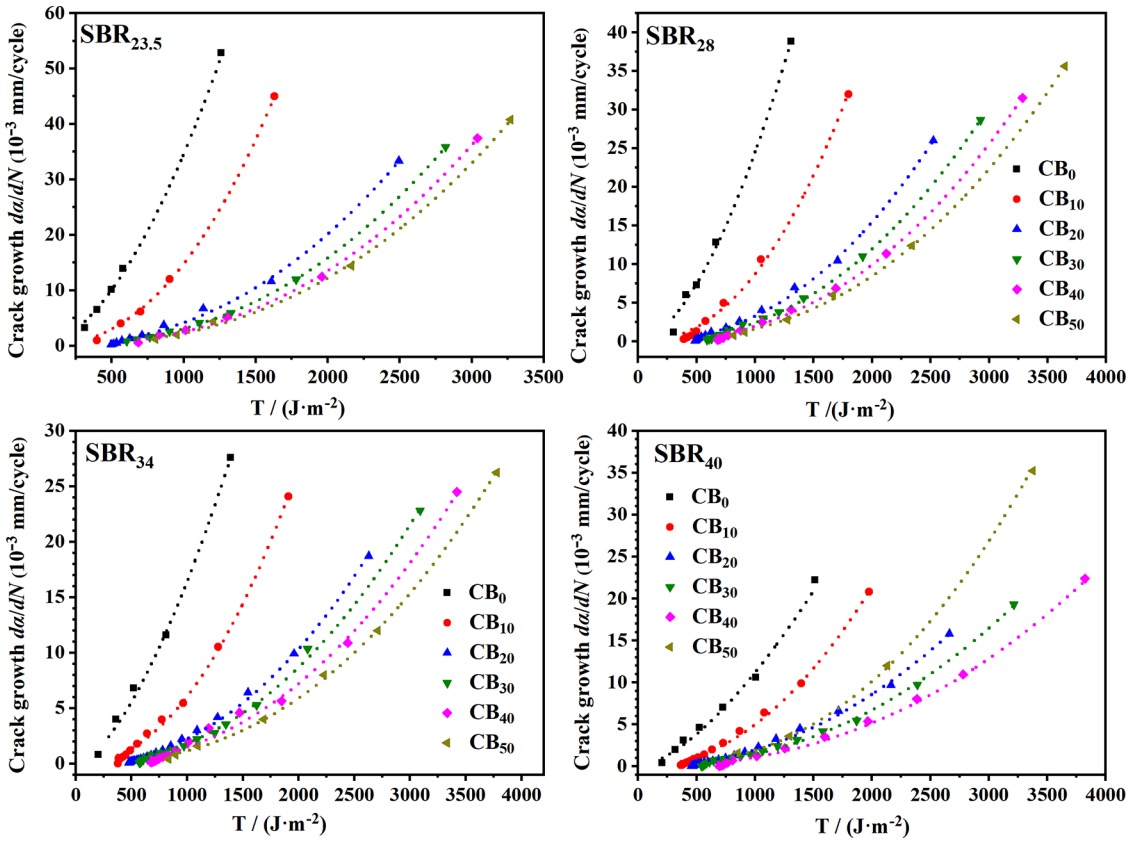

Figure 11. Fitting curve for the dynamic fatigue crack growth rate ($d\alpha/dN$) vs tearing energy (T) of SBR/CB with different CB contents.

Table 3. b Value for ($d\alpha/dN$) vs (T) of SBR/CB

sample	CB_0	CB_{10}	CB_{20}	CB_{30}	CB_{40}	CB_{50}
$SBR_{23.5}$	1.66×10^{-4}	2.18×10^{-6}	6.59×10^{-7}	2.40×10^{-7}	1.34×10^{-7}	1.07×10^{-7}
SBR_{28}	1.76×10^{-4}	1.91×10^{-6}	6.47×10^{-7}	3.24×10^{-7}	2.04×10^{-7}	1.37×10^{-7}
SBR_{34}	3.31×10^{-4}	2.27×10^{-6}	5.58×10^{-7}	3.49×10^{-7}	2.40×10^{-7}	1.32×10^{-7}
SBR_{40}	2.64×10^{-4}	2.42×10^{-6}	8.25×10^{-7}	3.48×10^{-7}	2.00×10^{-7}	1.16×10^{-7}

observed. For composites with CB, the b value is almost at the same level, the sensitivity of the crack growth rate to tearing energy can be known by the c value, and the larger the value is, the larger the variation in $d\alpha/dN$ with the change in tear energy. Figure 4 shows that the c value of the composite decreases with increasing styrene content, and the c value of the composite decreases first and then increases with increasing CB content. The c value of SBR_{40}/CB_{20} is the smallest (Table 4).

Table 4. c Value for ($d\alpha/dN$) vs (T) of SBR/CB

sample	CB_0	CB_{10}	CB_{20}	CB_{30}	CB_{40}	CB_{50}
$SBR_{23.5}$	1.77	2.28	2.27	2.37	2.42	2.44
SBR_{28}	1.71	2.24	2.22	2.29	2.33	2.36
SBR_{34}	1.57	2.20	2.14	2.24	2.27	2.32
SBR_{40}	1.54	2.13	2.10	2.21	2.25	2.41

The dynamic fatigue crack growth rate is related to the molecular structure of SBR and the content of CB. SBR is a random copolymer of styrene and butadiene. The styrene with a large volume on the molecular chain is the rigid component of SBR. When the tip of the dynamic fatigue crack meets the rigid group, it can produce a passivation effect on the crack tip and delay the development of the crack; thus, it can effectively suppress the growth of cracks when increasing the styrene content in SBR. CB is the reinforcing material of SBR, which can form a gel with rubber polymer and increase the strength of the matrix.[37] When the tip of the dynamic fatigue crack meets the gel formed by the CB particles, it can also suppress crack propagation or change the development direction of the crack, causing the development of the crack to be obviously slower. The rubber molecular chain restricted by CB particles is conducive to stress transfer, thus increasing the area of strain energy dissipation at the crack tip and expanding the influence range of styrene groups, producing a synergistic effect on fatigue life improvement. With the further increase in CB content, as mentioned above, the Payne effect of the composites increases, especially for SBR/CB with a high content of styrene; the interaction between CB and the rubber matrix is reduced, and the defects of CB agglomeration increase significantly, resulting in an increase in crack development due to stress concentration at defects of agglomeration. Therefore, with an increasing CB content, the fatigue life of SBR composites first increases and then decreases.

3.4. Dynamic Fatigue Failure Mechanism of SBR/CB Composites. *3.4.1. Dynamic Fatigue Fracture Analysis of*

https://doi.org/10.1021/acsomega.3c09872
ACS Omega 2024, 9, 2000−2011

SBR/CB Composites. Figures 12 and 13 show the initial crack growth section and the later crack growth section. Comparing

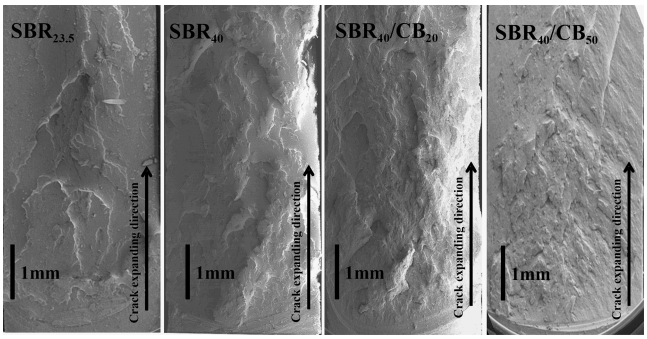

Figure 12. SEM images of the initial fracture surface after fatiguing.

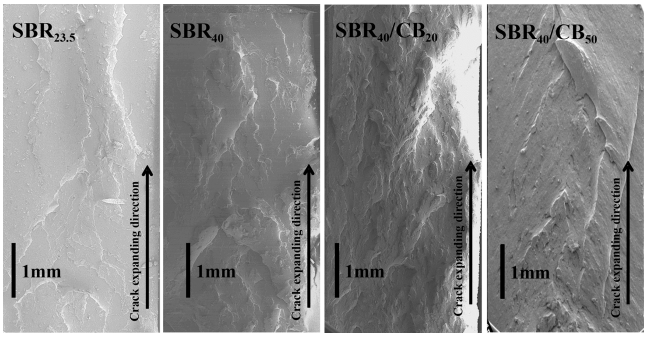

Figure 13. SEM images of the later fracture surface after fatiguing.

the fracture surface of the four materials, it is found that the initial and later sections of $SBR_{23.5}$ are relatively flat. The crack develops rapidly, the rubber base deformation is small,[38] and the fatigue fracture surface is smooth. The fracture surface of SBR_{40} is relatively rough, with large ups and downs in the early stage, and relatively flat in the later stage, which indicates that the rubber base deformation is relatively large in the fatigue process. The fatigue fracture surface changes from rough to smooth, and the crack growth rate increases greatly. The fatigue life of SBR_{40}/CB_{20} is the highest, the fracture surface is relatively rough in the early and late stages, and the crack growth rate is relatively low. However, the fatigue life of SBR_{40}/CB_{50} is greatly reduced because of CB agglomeration, and its fatigue cross section is so flat.

Figure 14 shows the fatigue section morphologies of SBR with different styrene contents and without CB. The fracture surface morphology of $SBR_{23.5}$ in the SEM image is relatively smooth. With increasing styrene content, the fracture surface becomes rougher.[38] The fracture face and edge of SBR_{40} are much rougher. The higher the styrene content, the more uneven the surface is, and after the initial smooth area, a smaller parabolic shape accompanied by uneven peaks and ravines can be observed clearly. In the early stage of the fatigue process, the rubber main crack tip produces a forced high-elastoplastic deformation, and the crack tip is passivated. When the matrix in front of the main crack tip reaches the crack initiation condition, new cracks are formed and expand, which are called secondary cracks. As shown in Figure 14, the initiation and propagation of the secondary cracks join into the expansion of the main crack to form many parabolic patterns.[38] In the fatigue process, the rubber matrix is deformed, as well as the parabolic shape.[39] As the incremental styrene content

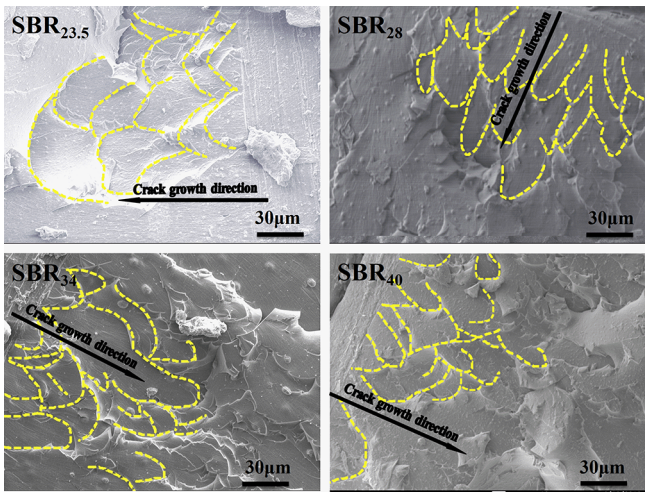

Figure 14. SEM images of the SBR/CB_0 fracture surface after fatigue.

increases, the more deformed parabolic the rubber fatigue fracture becomes. This is because styrene increases the rigidity of the rubber, which makes the work to be consumed during the expansion of the main crack along the prefabricated notch increase and slows down the expansion of the main crack. Meanwhile, when subjected to the same deformation load applied, the stress on the more rigid styrene portion will increase, and when the stress is greater than the critical extension stress of the microcrack, more microcracks will be formed in the area of stress concentration at the tip of the main crack. The initiation and propagation of many secondary cracks consume a large amount of strain energy.[40] Therefore, the increase of styrene content is favorable to consume more external stress work in the fatigue process, thus delaying the expansion of the main crack and improving the fatigue life of notched specimens.[41] Figure 15 shows the fatigue fracture morphology of the SBR_{40}/CB composites. As shown, when the CB content is 0 to 20 phr, the fatigue fracture roughness of the composite is higher, and the parabola morphology is more and less. When the CB content exceeds 20 phr, the fatigue fracture roughness of the composite decreases and the number of parabolic morphology declines with the further increase of CB content. The dynamic fatigue fracture of SBR_{40}/CB_{50} is relatively flat, and no parabolic pattern can be found on the fatigue fracture of SBR_{40}/CB_{50}.[42] CB in the rubber can increase the modulus and strain energy density of vulcanized rubber, which enhances the hysteresis loss during molecular chain segments moving. More importantly, CB in the SBR with high styrene content can dissipate a large amount of strain energy, which leads to the passivation, deflection, and branching of cracks, thus slowing down the development of cracks. However, excessive CB can easily lead to agglomeration, which makes it more difficult for the secondary cracks in rubber composite to initiate, and the expansion of primary cracks is easier.[43] When the CB content exceeds 40 phr, the interaction between rubber and CB is further weakened. Besides, CB agglomeration produces stress concentration, and the crack propagation work is reduced. The main crack propagation changes from secondary crack propagation to self-propagation driven by strain energy, which reduces the fatigue life.

3.4.2. Dynamic Fatigue Crack Tip Analysis of SBR/CB Composites. Figure 16 shows high-magnification images of the

https://doi.org/10.1021/acsomega.3c09872
ACS Omega 2024, 9, 2000−2011

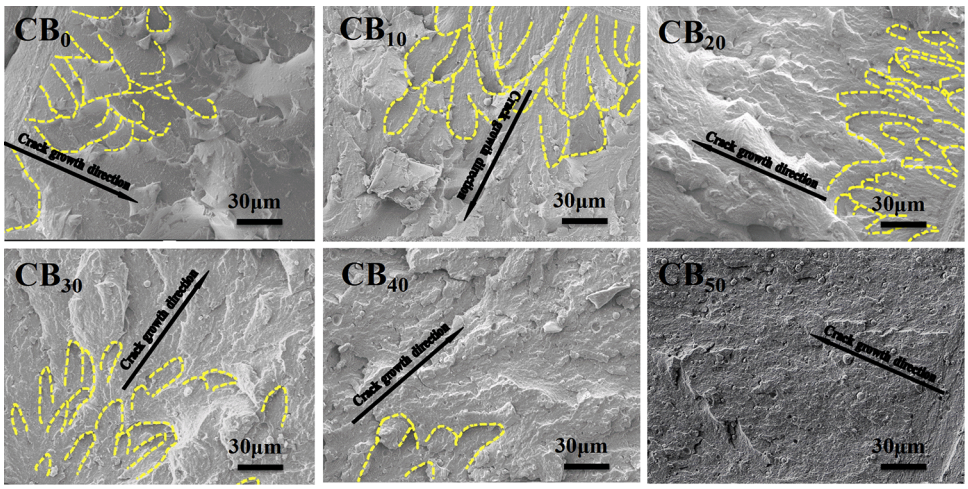

Figure 15. SEM images of the SBR_{40}/CB fracture surface after fatigue.

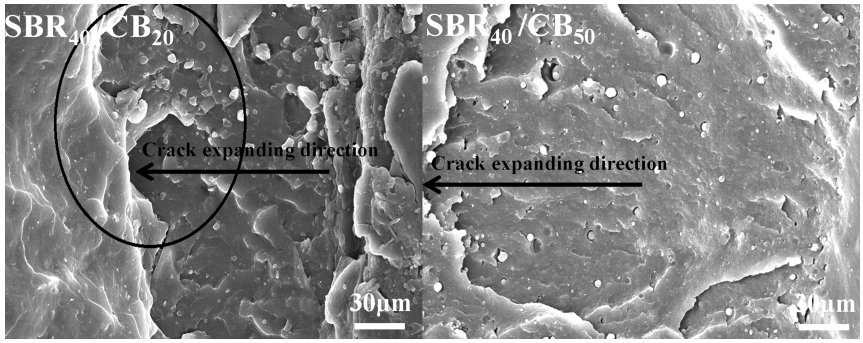

Figure 16. SEM images of the fatigue crack tip after dynamic fatigue.

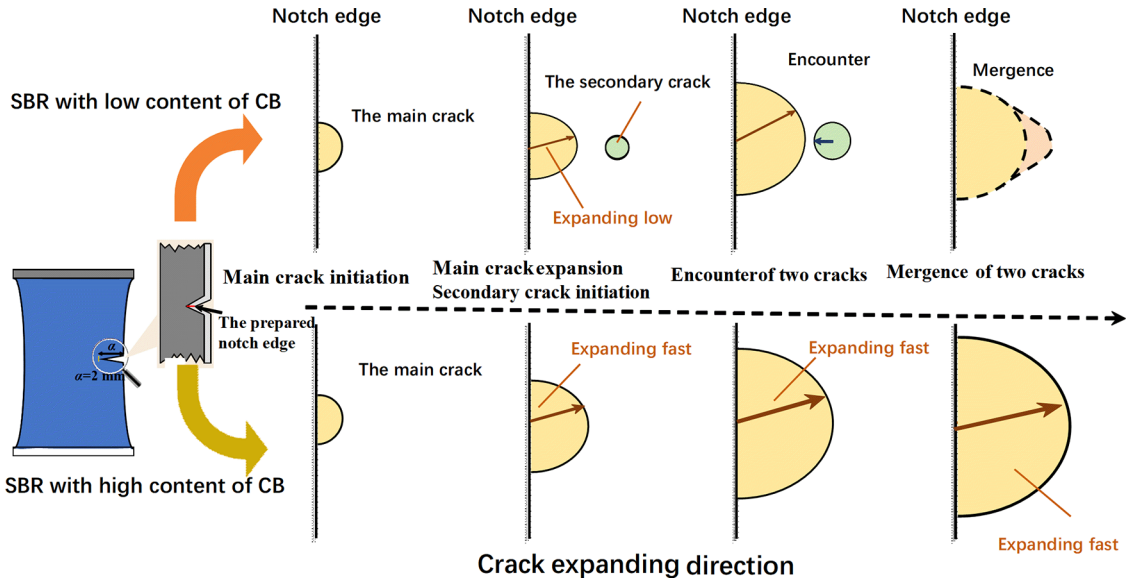

Figure 17. Schematic of crack expansion and formation of parabolic morphology for SBR/CB samples during dynamic fatiguing.

dynamic fatigue crack tips of SBR_{40}/CB_{20} and SBR_{40}/CB_{50}. The fatigue number of SBR_{40}/CB_{20} is 10,000 times, and the fatigue number of SBR_{40}/CB_{50} is 2500 times. Then, the notched samples are brittlely broken at low temperatures. From Figure 14, the zone near the crack tip of SBR_{40}/CB_{20} exhibits obvious hierarchical characteristics of the secondary crack source propagating around, but the zone near the crack tip of SBR_{40}/CB_{50} is smooth, and there is no obvious secondary crack feature. The matrix strength of SBR_{40}/CB_{20} is enhanced by CB, and the agglomeration of the filler is small. In the process of dynamic fatigue, a large number of secondary cracks are generated, a large amount of strain energy is consumed, and the development of the main crack is slow. In SBR_{40}/CB_{50}, the agglomeration of CB is serious due to the

https://doi.org/10.1021/acsomega.3c09872
ACS Omega 2024, 9, 2000−2011

weakened interaction between SBR and CB when both the contents of styrene are high, which leads to large defects caused by agglomeration. The main crack growth transformed into self-propagation driven by the strain energy, and the expansion rate increased.

Through the analysis of the dynamic fatigue fracture and crack tip, the rubber main crack enters a slow and steady growth stage in the early fatigue process and a secondary crack initiates and develops. The initiation and propagation of many secondary cracks consume a large amount of energy, which decreases the concentrated stress of the main crack tip and reduces the growth rate of the main crack. As shown in Figure 17, the two types of cracks merge and trace intersect, forming many parabolic shapes. For SBR with a high styrene content, more secondary cracks are generated in the front of the main crack tip and the development rate of secondary cracks is relatively slow. When the main crack and multiple secondary cracks meet, the parabola shape is small but the number is large, leading to the slow development of the main crack, and the parabola edge is rough. When a certain amount of CB is added to the SBR, the strength of the matrix is increased. The development of the main crack is suppressed when the gel formed by CB is encountered, resulting in a further decrease in the crack growth rate. However, with increasing CB content, the interaction between CB particles increases and the agglomeration of CB particles leads to a large increase in the size of defects. The superposition of the stress concentration of the main fatigue crack tip and the defects caused by the agglomeration of CB accelerate crack growth. There is not enough time to initiate many secondary cracks, leading to the main crack growth transforming from secondary crack propagation to self-propagation and the reduction of the fatigue life.

4. CONCLUSIONS

In this paper, an attempt was made to optimize the existing tread rubber system for engineering tires, and the synergistic effect of styrene and CB on the SBR was investigated. The internal rotation steric resistance of the molecular chain increased with the increasing styrene content so that the GTT of SBR was increased. The interaction between rubber macromolecules was reduced with the rising CB content so that the GTT of SBR/CB composites was decreased. The Payne effect and tan δ value increase were more obvious in the rubber composites with high styrene and CB contents, indicating that the interaction between the rubber matrix and CB was weakened, and the interaction between CB particles was enhanced. Since both the filler network formed by CB and styrene increase the rigidity of the rubber, the work required to be consumed during the extension of the main crack along the prefabricated notch increases, slowing the extension of the main crack. At the same time, because CB and styrene enhance the rigidity of the rubber part of the microzone, when subjected to the same deformation load applied, the stress on the rigid part of the material will increase, and when the stress is greater than the critical extension stress of the microcrack, more microcracks will be formed in the area of stress concentration at the tip of the main crack. Parabola patterns were formed on the fatigue fracture surface by the trace intersection of the main and secondary cracks. The formation of more parabolas represents the creation of more microcracks at the crack front, and this process absorbs a large amount of energy, further slowing the expansion of the main crack and extending the material life. This synergistic effect of styrene and CB can significantly improve the fatigue life of the rubber material. This synergistic effect was most obvious when the CB content was 20 phr and the styrene content was 40%. The fatigue life of SBR_{40}/CB_{20} was 868% longer than that of $SBR_{23.5}$. However, with a further increase in the CB content, the superposition of the stress concentration of the main fatigue crack tip and the defects caused by the agglomeration of CB accelerated the crack growth. Thus, the main crack propagation changed from secondary crack propagation to self-propagation driven by strain energy, the rate of crack propagation increased, and the number of secondary cracks decreased, leading to a reduction in the fatigue life. This study provided a new idea to further improve the service life of tires under the existing tire tread rubber system.

AUTHOR INFORMATION

Corresponding Author

Zhu Luo − *College of Materials and Metallurgy, Guizhou University, Guiyang 550025, China;* orcid.org/0000-0001-8848-9354; Email: luozhu2000@sina.com

Authors

Li'e Wang − *College of Materials and Metallurgy, Guizhou University, Guiyang 550025, China; Guizhou Tire Co. Ltd., Guiyang 550207, China*

Le Yang − *School of Materials and Energy Engineering, Guizhou Institute of Technology, Guiyang 550025, China*

Jincheng Zhong − *School of Materials and Architectural Engineering, Guizhou Normal University, Guiyang 550001, China*

Yinhan Xu − *College of Materials and Metallurgy, Guizhou University, Guiyang 550025, China*

Complete contact information is available at: https://pubs.acs.org/10.1021/acsomega.3c09872

Notes

The authors declare no competing financial interest.

ACKNOWLEDGMENTS

This work was financially supported by National Natural Science Foundation of China, and the Grant/Award Number is 51763004.

REFERENCES

(1) Morishita, Y.; Tsunoda, K.; Urayama, K. Crack-tip shape in the crack-growth rate transition of filled elastomers. *Polymer.* **2017**, *108*, 230−241.

(2) Zhang, H.; Scholz, A. K.; De Crevoisier, J.; Berghezan, D.; Narayanan, T.; Kramer, E. J.; Creton, C. Nanocavitation around a crack tip in a soft nanocomposite: A scanning microbeam small angle X-ray scattering study. *J. Polym. Sci., Part B: Polym. Phys.* **2015**, *53*, 422−429.

(3) Bouchbinder, E.; Fineberg, J.; Marder, M. Dynamics of Simple Cracks. *Annu. Rev. Conden. Ma. P.* **2010**, *1*, 371−395.

(4) South, J. T.; Case, S. W.; Reifsnider, K. L. Crack growth of natural rubber using a modified double cantilever beam. *Mech. Mater.* **2002**, *34*, 451−458.

(5) Horst, T.; Heinrich, G. Crack propagation behavior in rubber materials. *Polym. Sci. Ser.* **2008**, *50*, 583−590.

(6) Lake, G. J.; Yeoh, O.; H. Effect of crack tip sharpness on the strength of vulcanized Rubbers. *J. Polym. Sci., Polym. Chem.* **1987**, *25*, 1157−1190.

https://doi.org/10.1021/acsomega.3c09872
ACS Omega 2024, 9, 2000−2011

(7) Livne, A.; Bouchbinder, E.; Fineberg, J. Breakdown of linear elastic fracture mechanics near the tip of a rapid crack. *Phys. Rev. Lett.* **2008**, *101*, No. 264301.
(8) Persson, B. N. J.; Brener, E. A. Crack propagation in viscoelastic solids. *Phys. Rev. E* **2005**, *71*, No. 036123.
(9) Le Cam, J. B.; Huneau, B.; Verron, E.; Gornet, L. Mechanism of fatigue crack growth in carbon black filled natural rubber. *Macromolecules.* **2004**, *37*, 5011−5017.
(10) Garbone, G.; Persson, B. N. J. Hot cracks in rubber: origin of the giant toughness of rubberlike materials. *Phys. Rev. Lett.* **2005**, *95*, No. 114301.
(11) Knauss, W. G. A review of fracture in viscoelastic materials. *Int. J. Fract.* **2015**, *196*, 99−146.
(12) Chudnovsky, A.; Moet, A. A theory for crack layer propagation in polymers. *J. Elastom. Plast.* **1986**, *18*, 50−55.
(13) Kaang, S.; Jin, Y. W.; Huh, Y.; Lee, W. J.; Im, W. B. A test method to measure fatigue crack growth rate of rubbery materials. *Polym. Test.* **2006**, *25*, 347−352.
(14) Chudnovsky, A.; Moet, A. Thermodynamics of translational crack layer propagation. *J. Mater. Sci.* **1985**, *20*, 630−635.
(15) Maiti, A.; Small, W.; Gee, R. H.; Weisgraber, T. H.; Chinn, S. C.; Wilson, T. S.; Maxwell, R. S. Mullins effect in a filled elastomer under uniaxial tension. *Phys. Rev. E* **2014**, *89*, No. 012600.
(16) Diani, J.; Fayolle, B.; Gilormini, P. A review on the Mullins effect. *Eur. Polym. J.* **2009**, *45*, 601−612.
(17) Lake, G. J. Fatigue and fracture of elastomers. *Rubber Chem. Technol.* **1995**, *68*, 435−460.
(18) Persson, B. N. J.; Albohr, O.; Heinrich, G.; Ueba, H. Crack propagation in rubber-like materials. *J. Phys-Condens. Mater.* **2005**, *17*, R1071.
(19) Ramier, J.; Gauthier, C.; Chazeau, L.; Stelandre, L.; Guy, L. Payne effect in silica-filled styrene-butadiene rubber: influence of surface treatment. *J. Polym. Sci., Polym. Phys.* **2007**, *45*, 286−298.
(20) Dong, B.; Liu, C.; Zhang, L. Q.; Wu, Y. P. Preparation, fracture, and fatigue of exfoliated graphene oxide/natural rubber composites. *RSC Adv.* **2015**, *5*, 17140−17148.
(21) Dong, B.; Liu, C.; Wu, Y. P. Fracture and fatigue of silica/carbon black/natural rubber composites. *Polym. Test.* **2014**, *38*, 40−45.
(22) Dong, B.; Liu, C.; Lu, Y. L.; Wu, Y. P. Synergistic effects of carbon nanotubes and carbon black on the fracture and fatigue resistance of natural rubber composites. *J. Appl. Polym. Sci.* **2015**, *132*, 42075.
(23) Weng, G. S.; Chang, A. J.; Fu, K. R.; Kang, J.; Ding, Y. X.; Chen, Z. R. Crack growth mechanism of styrene-butadiene rubber filled with silica nanoparticles studied by small angle X-ray scattering. *RSC Adv.* **2016**, *6*, 8406−8415.
(24) Weng, G. S.; Yao, H.; Chang, A. J.; Fu, K. R.; Liu, Y. P.; Chen, Z. R. Crack growth mechanism of natural rubber under fatigue loading studied by a real-time crack tip morphology monitoring method. *RSC Adv.* **2014**, *4*, 43942−43950.
(25) Weng, G. S.; Huang, G. S.; Lei, H. X.; Qu, L. L.; Nie, Y. J.; Wu, J. R. Crack initiation and evolution in vulcanized natural rubber under high temperature fatigue. *Polym. Degrad. Stab.* **2011**, *96*, 2221−2228.
(26) Yin, Q. Y.; Wang, L. T.; Cao, X. J.; Ding, Y. X.; Weng, G. S. Influence of grafted silica particles on the crack growth behavior of solution polymerized butadiene styrene rubber. *Polym. Mater. Sci. Eng.* **2017**, *33*, 167−171.
(27) Fu, K.; Weng, G. S.; Yan, Z. J.; Chen, Z. R.; Yin, Q. Y.; Zhu, M. Q. Crack growth mechanism of fumed silica filled natural rubber. *Polym. Mater. Sci. Eng.* **2016**, *32*, 9095.
(28) Yang, B.; Li, P.; Luo, Z.; Zhong, J. C.; Yin, L. P. Influence of thermal oxidation and maleinized liquid polybutadiene on dynamic and static performance of short aramid fiber-reinforced carbon black-ethylene propylene diene monomer composites. *Polym. Compos.* **2020**, *41*, 2036−2045.
(29) Zhong, J. C.; Luo, Z.; Yang, L.; Sheng, X.; Li, X. L.; Yin, L. P.; Yang, B. Construction of an in situ interfacial layer for aramid fiber reinforced styrene butadiene rubber composites. *J. Appl. Polym. Sci.* **2020**, *137*, 49420.
(30) Luo, Z.; Chen, W. L.; Jin, Z.; Dong, F. P.; Yang, L.; Zheng, Q. Epoxy resin modified maleic anhydride-grafted-liquid polybutadiene on the properties of short aramid fiber reinforced natural rubber composite. *Polym. Compos.* **2018**, *39*, 2006−2015.
(31) Yin, L. P.; Zhou, Z. T.; Luo, Z.; Zhong, J. C.; Li, P.; Yang, B.; Yang, L. Reinforcing effect of aramid fibers on fatigue behavior of SBR/aramid fiber composites. *Polym. Test.* **2019**, *80*, No. 106092.
(32) Kaynak, N.; En, S. Effect of feldspar filler on physical and dynamic properties of SBR/CB based tire tread compounds: Effect of addition method of silane coupling agent. *J. Elastom. Plast.* **2021**, *53*, 525−551.
(33) Li, H. Y.; Zong, X.; Li, N.; Zhang, X. P.; He, A. H. Influences of crosslinkable crystalline copolymer on the polymer network and filler dispersion of NR/ESBR/CB nanocomposites. *Compos. Part A-Appl. S.* **2021**, *140*, No. 106194.
(34) Rivlin, R. S.; Thomas, A. G. Rupture of rubber. I. Characteristic energy for tearing. *J. Polym. Sci.* **1953**, *10*, 291−318.
(35) Grosch, K. Rolling resistance and fatigue life of tires. *Rubber Chem. Technol.* **1988**, *61*, 42−46.
(36) Gan, S. C.; Wu, Z. L.; Xu, H. L.; Song, Y. H.; Zheng, Q. Viscoelastic behaviors of carbon black gel extracted from highly filled natural rubber compounds: Insights into the Payne Effect. *Macromolecules.* **2016**, *49*, 1454−1463.
(37) Medalia, A. I. Effective degree of immobilization of rubber occluded within carbon-black aggregates. *Rubber Chem. Technol.* **1972**, *45*, 1171−1194.
(38) Du, P. H.; Xue, B.; Song, Y. H.; Lu, S. J.; Yu, J.; Zheng, Q. Fracture surface characteristics and impact properties of poly (butylene terephthalate). *J. Polym. Bull.* **2010**, *64*, 185−196.
(39) Stéphanie, B.; Huneau, B.; Verron, E. In-situ SEM study of fatigue crack growth mechanism in carbon black filled natural rubber. *J. Appl. Polym. Sci.* **2010**, *117*, 1260−1269.
(40) Le Cam, J. B.; Huneau, B.; Verron, E.; Gornet, L. Mechanism of fatigue crack growth in carbon black filled natural rubber. *Macromolecules* **2004**, *37* (13), 5011−5017.
(41) Verron, E.; Huneau, B.; Beurrot, S. In-situ SEM study of fatigue crack growth mechanism in carbon black-filled natural rubber. *J. Appl. Polym. Sci.* **2016**, *117*, 1260−1269, DOI: 10.1002/app.31707.
(42) Ji, X. W.; Zhang, X.; Yue, J. L.; Lu, Y. L.; Zhang, L. Q. Comparative study on the effect of carbon nanotubes and carbon black on fatigue properties of natural rubber composites. *Int. J. Fatigue.* **2022**, *163*, No. 107094.
(43) Saintier, N.; Cailletaud, G.; Piques, R. Cyclic loadings and crystallization of natural rubber: An explanation of fatigue crack propagation reinforcement under a positive loading ratio. *Mater. Sci. Eng. A-Struct.* **2011**, *528* (3), 1078−1086.

https://doi.org/10.1021/acsomega.3c09872
ACS Omega 2024, 9, 2000−2011